Journal of Hydroscience and Hydraulic Engineering
Vol.12, No.2, November, 1994, 101-112

HEAT ENVIRONMENT IN A SUMMER DAY AT SURROUNDING REGION OF AN URBAN RIVER

by

S. Takewaka
Dept. of Civil Eng., Kyushu University, Fukuoka, Japan

S. Ikeda
Dept. of Civil Eng., Tokyo Institute of Technology, Tokyo, Japan

T. Hirayama
Public Works Research Institute, Tsukuba, Japan

Y. Kayaba
Public Works Research Institute, Tsukuba, Japan

and

T. Zaitsu
Graduate School, Tokyo Institute of Technology, Tokyo, Japan

SYNOPSIS

Meteorological field observations were conducted at Ara-river(Tokyo) in a summer season to evaluate the microclimate around the river course. The observation consists of (i) measurements on wind velocity, temperature and relative humidity (vapor density) profiles across the river course by using captive balloons up to height of $60m$, and (ii) measurements on momentum, heat and vapor fluxes performed on the flood plain and the water body. The development of internal boundary layers on the vegetated flood plain and the water body accompanied with cooling of the atmosphere were observed, which extended to a height of $30m$ at maximum. The role of the flood plain and the water body in heat exchanging process are discussed based on the results of the flux measurements and heat balance analyses.

INTRODUCTION

A considerable amount of studies indicate the existence of heat island which is meteorological phenomenon formed over large cities and suburban areas (e.g. Ref. 1). Its remarkable effect on the climate is the increase of temperature in urbanized area compared with that in suburbs. In the large cities of Japan, the effect of heat island is strong and an uncomfortable heat environment is formed, which produces inconvenience in the urban daily life in summer seasons (e.g. Ref. 2).

Among several ideas to improve the heat environment, the control of urban climate using vegetated area and water body have been proposed (e.g. Ref. 3). Their effect and process on the improvement of the urban heat environment, however, are not fully understood quantitatively and the idea is still remained conceptual.

The present study focuses on a small-scale climate in surrounding region of a urban river in a summer season. A detailed meteorological observation was conducted at Ara-river in Tokyo. The heat exchange process between the atmosphere and the river course, and the amounts of atmospheric cooling are explained based on the measurements.

Table 1 Instrumentation of the observation

captive balloon (location : $a1 \sim a4$)

variable	height $z(m)$	instrumentation	notice
U	1, 2, 5, 10, 15, 20, 30, 40, 50, 60	cup anemometer	*1
T	50, 40, 30, 20, 15, 10, 5, 2, 1	Pt resistance	
RH		polymer capacity	

flood plain (location : b)

variable	height $z(m)$	instrumentation	notice
U,WD	2.1	propeller anemometer	*2
U	0.2, 0.4, 0.8, 1.6, 2.8, 5	hot-wire anemometer	
T	0.2, 0.6, 1.2	Pt resistance	
RH	0.2, 0.6, 1.2	polymer capacity	
R_{net}	1.75	net radiometer($0.3 \sim 30\mu m$)	
$S_R \downarrow$	1.83	solarmeter($0.3 \sim 2.8\mu m$)	
G_{soil}	-4, -12, -21 (cm)	heat flux plate	
θ, u, v, w	0.85	ultra sonic anemometer	*3
T_s		infrared radiometer	
T_{soil}	-1, -3, -5, -10, -15, -25, -40 (cm)	thermistor	

water surface (location : c)

variable	height $z(m)$	instrumentation	notice
U	1.25, 2.25	hot-wire anemometer	*4
T	1.25, 2.25	Pt resistance	
RH	1.25, 2.25	polymer capacity	
T_{sw}		infrared radiometer	
T_{water}	-0.5, -1, -2, -3	thermistor	

*1 : Balloons were started to measure at 00min of every hour. Data were collected at every height with sampling rate of $1Hz$, and the averaged value was taken for 1 minute-average. 25 minutes were required for one operation.

*2 : Data were collected continuously with sampling rate of $0.25Hz$. The sampled signals were reduced to 25 minutes average from 00–25min and 30–55min of every hour.

*3 : θ = air temperature, u, v, w = three components of wind velocity. Data were collected during 00–40min of every hour with sampling rate of $20Hz$. The correlation of θ and vertical velocity v fluctuations were calculated for 25 minutes average ($-\overline{v'\theta'}$).

*4 : Data were collected continuously with sampling rate of $1Hz$. The sampled signals were averaged for 25 minutes measurement, i.e. from 00–25min and 30–55min of every hour.

METEOROLOGICAL OBSERVATION IN A RIVER COURSE

Set-up of the meteorological observation and the weather condition

Meteorological observation was conducted on July 29th, 1992 (5:00–20:30h), at Ara-river, which flows through the western part of the metropolitan area of Tokyo in Kanto plain. The location of the observation site was about $13km$ north of Tokyo bay. On the day of the observation, the Kanto plain was covered with a pacific high pressure, which is a typical weather condition for post rainy season in Japan. The weather was fine throughout the day, and land breeze and sea breeze were observed in the morning and in the afternoon, respectively.

The plan view and the cross section of the observation site are shown in Fig. 1. The width of the flood plains on both sides of the river banks and the width of the water body are approximately $100m$ and $200m$, respectively. Almost all of the surfaces of the flood plains were

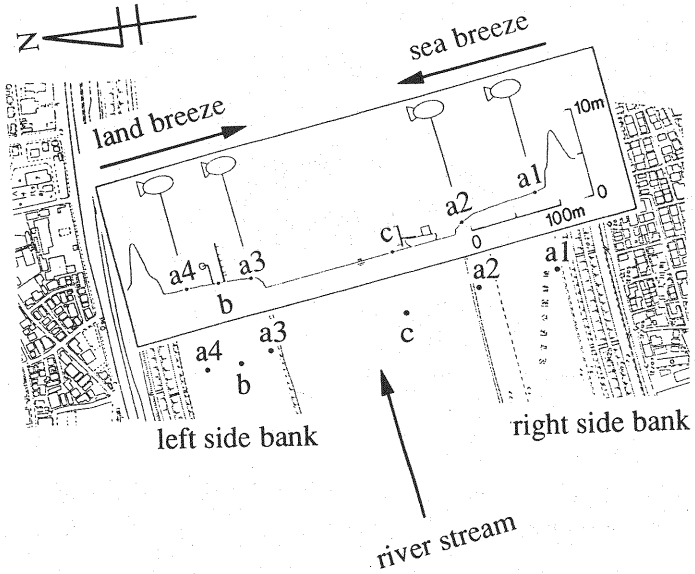

Fig. 1 Location of the observation site and setup of the instruments.

covered with short grasses. Levee of $6m$ height separates the river course from the surrounding city region. The average height of the buildings in the city region is the same as that of the levee.

The variables observed and the instrumentation used are listed in Table 1. All instruments used to measure the temperature were calibrated in the laboratory prior to the observation.

The vertical profiles of wind speed, temperature and relative humidity up to 60 m were measured at locations $a1 \sim a4$ using captive balloons, the location of which is depicted in Fig.1. The operation of the 4 balloons were synchronized by radio communication. A cycle of the observation using balloons started at $00min$ of every hour, and it took approximately 25 minutes to complete one operation. The elevation of measurements are listed in Table 1.

The instrumentations for the measurement of heat balance were placed on the flood plain (location b in Fig.1), from which detailed profiles of wind speed, temperature and relative humidity near the ground surface were obtained with a mini-tower of $5m$ height. The short-wave solar radiation, the long-wave radiation from the sky and the long-wave radiation from the flood plain were detected, and the temperature and heat flux in the soil layers were also measured (see Table 1).

A boat was moored at location c on the water body, where wind velocity, temperature of air and water and relative humidity were measured.

The diurnal variations of wind speed, wind direction, temperature and vapor density observed at location b on the flood plain are shown in Fig. 2. Vapor density ($= q \ \ g/m^3$) is calculated from the measured air temperature ($= T \ \ ^\circ C$) and relative humidity ($= RH$ in %) employing the following relation (see e.g. Bolton (4)) :

$$q = \frac{RH}{100} \times \frac{217}{T + 273.15} \times 6.112 \, exp \, \frac{17.67 \, T}{T + 243.5} \tag{1}$$

The air temperature shows a diurnal variation with its maximum value of $35^\circ C$ at noon. The variation of the vapor density, however, is very small, and it was almost constant throughout the day (Fig. 2). The change of wind direction indicates that the weather condition of the observation day can be divided into three conditions A, B and C as follows :

- Land breeze period; A (5–10h) : wind direction is north, and it comes from the Kanto plain.
- Calm period; B (10–13h) : weak wind with variable wind direction.

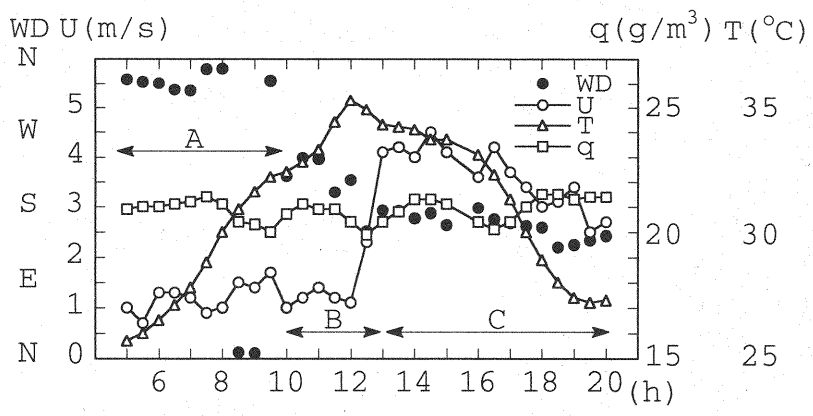

Fig. 2 Diurnal variation of the wind speed U, wind direction WD, temperature T and vapor density q observed at location b on the flood plain.

• Sea breeze period; C (13–20h) : wind direction is south, and it comes from the Tokyo bay. The wind crosses the river course with the right angle during the period, A and C.

Development of an internal boundary layer across the river course

The vertical profiles of wind speed (= U), temperature (= T) and vapor density (=q) measured with the captive balloons at location $a1 \sim a4$ are shown in Fig. 3, in which z = vertical coordinate taken positive upward from the surface of the flood plain. Distinct developments of internal boundary layers were observed in the land breeze time(Fig. 3a) and sea breeze time(Fig. 3c). The features of the air flow above the river course are described in the following :

• Land breeze period; A (Fig. 3a) : The northern wind from the city region accelerates in the river course, which was caused by the difference of the surface roughness between the city region and the river course. The temperature profile indicates that the lower air near the surface was cooled over the left side flood plain and the water surface, and then it was heated slightly over the right side flood plain. The temperature at $z = 5m$ was decreased by $0.5°C$ while the air crossed the river course. No distinct change of vapor density profile was observed in the downwind direction, except that they were relatively higher near the surface.

• Calm period; B (Fig. 3b) : The wind was weak and the vertical distribution is almost uniform. Steep gradient were observed for the air temperature near the ground surface. The temperature and the vapor density above the river course were uniform above $z = 10m$.

• See breeze period; C (Fig. 3c) : The lower layer of the atmosphere was again accelerated, and it was cooled above the river course in a similar manner as described previously. The temperature profile reveals that the cooled layer extends to a height of $30m$, forming an almost neutral stratification. The temperature at $z = 5m$ was decreased by $0.8°C$ while the air crossed the river course. Vapor density of the lower atmosphere increased above the water surface, whereas its downwind variation of vertical profiles above the flood plains was very small.

The observed temperature above $z = 30m$ at location $a2$ were always higher than that of observed at location $a1$ in the period C. The rise of the temperature at the elevation seems to be significant, because it ($\simeq 0.4°C$) exceeds the official accuracy of the thermometer ($\pm 0.3°C$). This phenomenon, however, is difficult to explain from a viewpoint of the development of two dimensional internal boundary layer in the river course.

The temperature of the adjacent city region was observed to be decreased by the intrusion of the cooled air layer from the river course. The extent to which the cooling effect of the river reaches depends on the heat exchange rate of the cooled air layer with the city region (Ref. 5).

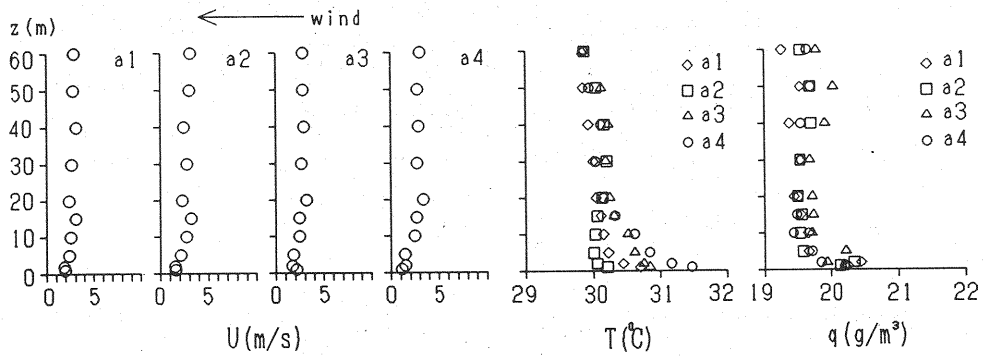

(a)

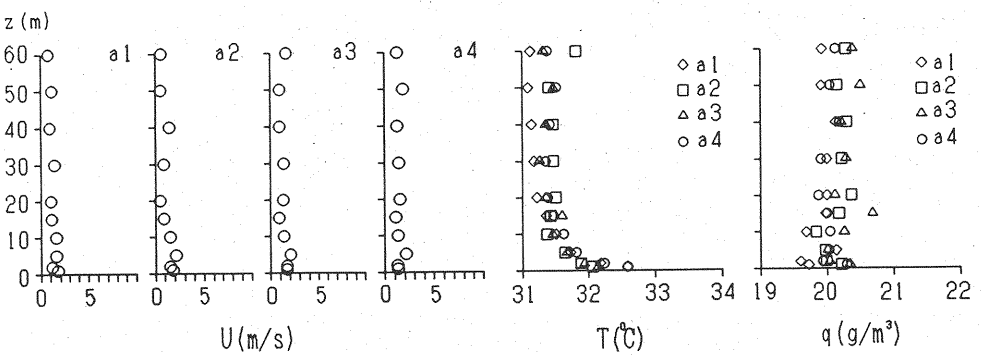

(b)

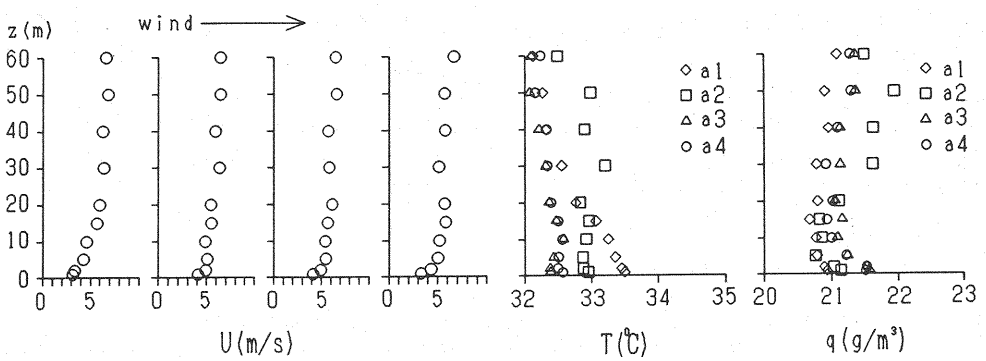

(c)

Fig. 3 Vertical profiles of wind speed, temperature and vapor density across the river course at: (a) $9h$, (b) $10h$, (c) $14h$.

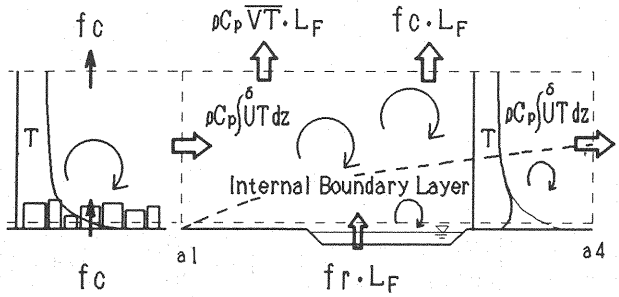

Fig. 4 Estimation of F' above the river course.

Heat exchange between the atmosphere and the river course

While the wind crosses the river course, the temperature of the lower atmosphere is decreased remarkably as described in the previous section. In this section, the temperature decrease in downwind direction, namely the amount of heat exchange between the atmosphere and the river course (= flood plain + water body) is estimated by accounting the heat–flux balance within a space above the river course.

The amount of heat exchange F', is calculated from the distributions of U and T obtained at the location $a1$ and $a4$.

$$F' = \frac{\rho C_p}{L_F} \int_0^{\delta} (U_d T_d - U_u T_u) dz \tag{2}$$

where ρ = air density, C_p = specific heat for constant pressure, L_F = fetch distance between station $a1$ and station $a4$, δ = upper integral limit, and the subscripts d and u denote that they are the values measured at the downwind and the upwind location, respectively (see Fig. 4).

To estimate the value of F', we assumed that the phenomenon is uniform along the longitudinal direction of the river course. It is assumed further that the air flow reaches equilibrium vertical profiles of wind speed and temperature above the city region. Therefore, the sensible heat flux at the ground ($= f_c$) is equal to the sensible heat flux at the upper boundary of the control volume as shown in Fig. 4, in which the boundaries of the control volume are depicted by broken lines. In the river course, the sensible heat flux at the bottom surface is denoted with f_r. The sensible heat flux at the upper boundary can be regarded as f_c, if the boundary is taken far outside the internal boundary layer, which develops from the upwind boundary of the river course. Considering the balance of heat which passes through the boundaries, the following relationship is obtained.

$$F' = F - \rho C_p \overline{VT}; \quad F = f_r - f_c \tag{3}$$

where V = vertical wind velocity and $-\rho C_p \overline{VT}$ = the average of the heat flux at the upper boundary transported by the vertical (downward) flow induced to compensate the acceleration of the flow in the inner boundary layer above the river course. Eq. 3 suggests that the value F' estimated with Eq. 2 includes the effect of sensible heat fluxes difference at the bottom surface inside and outside the river course ($F = f_r - f_c$), and the effect of downward flow($-\rho C_p \overline{VT}$).

The amount of heat exchange which relates to F is estimated herein for every one hour. Eq. 2 was calculated using the averaged value of U_d and U_u at each elevation. This procedure excludes the effect of air flow acceleration in the river course, and extracts only the amount of heat exchange due to the sensible heat fluxes difference. The height of the upper boundary, δ, was taken to be $30m$, which is the the inner boundary layer thickness determined from the observed temperature profiles. The calculated F increased slightly if δ was taken a larger value.

The diurnal variation of F thus estimated is depicted in Fig. 5 (data lack in the period B, because the wind direction changed frequently, and the inner boundary layer was not clearly formed). The amount of heat exchange takes maximum (F became minimum) at the time $13h$. The rate of heat exchange was large in the afternoon compared with it in the morning. From

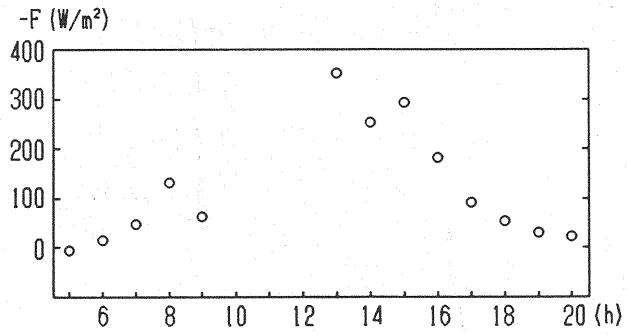

Fig. 5 Diurnal variation of F estimated between $a1$ and $a4$.

this result, we can expect that the effect of cooling of the river on air flow becomes large in the afternoon.

Heat balance on the flood plain and the water body

This section presents the results of the heat balance analysis on the flood plain(location b) and the water body(location c). The balance of heat fluxes on the the surfaces was studied by using the following equation (Ref. 6a):

$$R_{net} = H + \ell E + G \tag{4}$$

where H = sensible heat flux, ℓE = latent heat flux and G = heat flux below the surfaces, where the fluxes away from the surface are taken to be positive. H is equivalent to f_c and f_r which appeared in the previous section and G indicates the heat flux into soil or water body. The left side of Eq. 4 is the net radiative energy flux described by

$$R_{net} = (1 - \alpha)S_R \downarrow + L_R \downarrow - \sigma T_s^4 \tag{5}$$

where, $S_R \downarrow$= downward short–wave radiation (= solar radiation), $L_R \downarrow$= downward long–wave radiation, α = albedo of the surface, T_s = surface temperature, σ = Stefan–Boltzman constant and σT_s^4 = upward long–wave radiation emitted from the surface. Here, the fluxes towards the surface are taken to be positive.

(i) Heat balance on the flood plain

The components of net radiation R_{net} were measured on the flood plain, in which the sensible heat flux H and the latent heat flux ℓE were determined with the mean profile method (Ref. 6b) using the vertical profiles of wind, temperature and vapor density obtained at the mini–tower. Figure 6 shows an example of the observed profiles. The frictional velocity, the frictional temperature and the frictional vapor density were determined by fitting the universal functions to the measured values, and the results of best–fitting are depicted by solid lines in the figure. The value of H estimated from the profile method was compared with the vertical sensible heat fluxes (= H_u, see Fig.7 indicated later) measured directly with a ultra sonic anemometer applying the eddy correlation method (Ref. 6c). H and H_u show good agreement in the period A and C. A small discrepancy appears in the period B, during which the development of the inner boundary layer was insufficient. During this period, the application of the profile method was inappropriate, and the estimation of H and ℓE became inaccurate. The sensible heat flux into the ground by conduction G was determined both from the variation of temperature with time and direct measurement of heat flux in the soil layer.

The diurnal variation of heat balance on the flood plain thus obtained is shown in Fig. 7. The sensible heat flux H did not exceed 100 W/m^2 during the day. Most part of the net radiation R_{net} is balanced with latent heat flux ℓE, which indicates that the net radiation is consumed by the evapotranspiration from the vegetation and the bare soil surface.

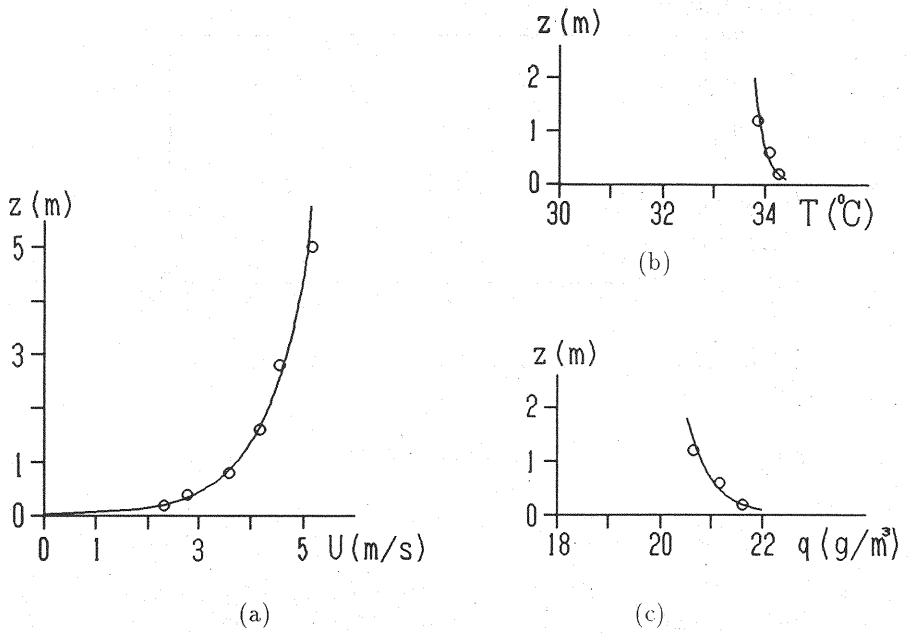

Fig. 6 Vertical profiles of (a) wind speed, (b) temperature and (c) vapor density on the location b at the time $14h$. The circles indicate the observed values and the solid lines show the fitted universal functions (Ref. 6b).

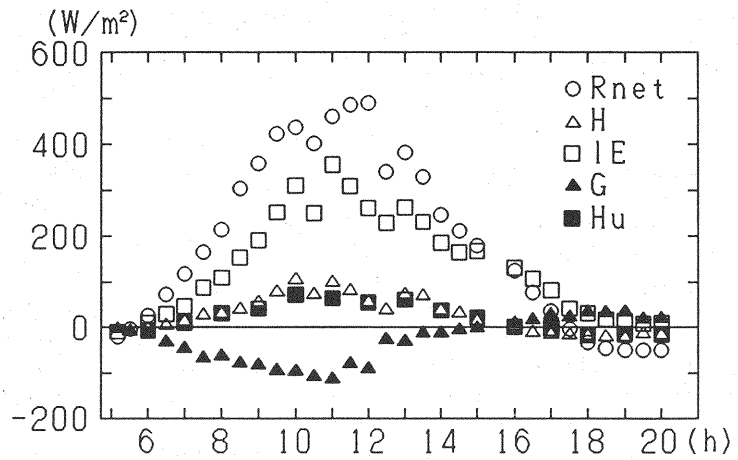

Fig. 7 Heat balance on the flood plain. The sign of G is reversed. Negative values mean that the heat is conducted into the ground.

(ii) Heat balance on the water body

The measurements on the water body were simplified compared with those on the flood plain, because the installation of the instruments was restricted on the boat. The wind speed, the temperature, the vapor density and the water surface temperature ($= T_{sw}$) observed on the water body are depicted in Fig. 8. The net radiation on the water body was estimated from the following quantities : (1) water surface temperature, from which the upward long-wave radiation was calculated using the Stefan–Boltzman formula, (2) albedo of the water, which is assumed

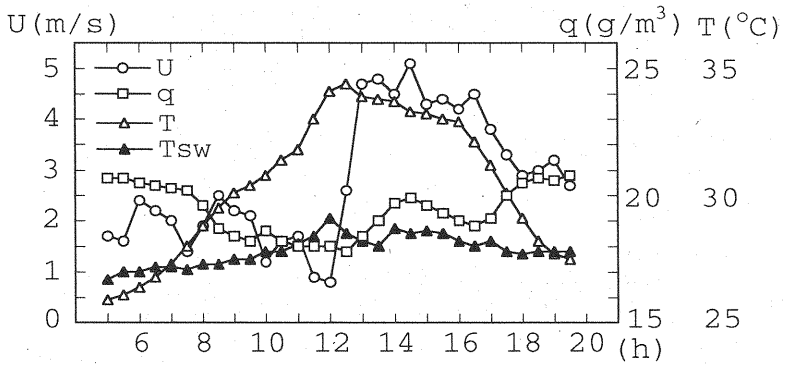

Fig. 8 Diurnal variation of mean wind speed U, mean temperature T, and mean vapor density q above the water body ($z = 1.5m$), and water surface temperature T_{sw}.

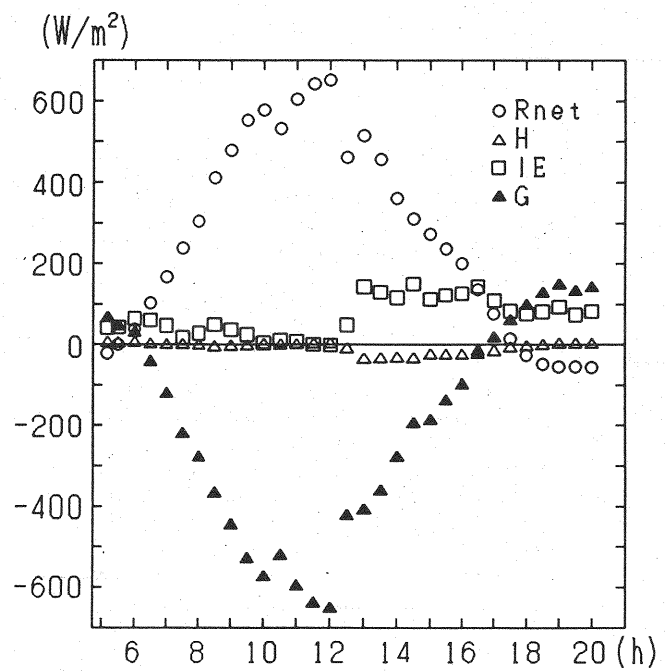

Fig. 9 Heat balance on the water body. The sign of G is reversed. Negative values mean that the heat is stored in the water body.

to be $\alpha = 0.07$ (Ref. 6a) and (3) the downward radiations, $S_R \downarrow$ and $L_R \downarrow$ measured on the flood plain. The sensible heat flux and latent heat flux were estimated by the bulk method (Ref. 6b), using the water surface temperature, the wind speed, the temperature and the vapor density measured on the boat. The component of the heat balance still remained unknown is G, which consists of the vertical convection and conduction of sensible heat toward deeper layer of the river, and the solar radiation penetrated into the water body . The direct evaluation of G from the obtained data was very difficult, and therefore it is evaluated as a residual of the heat balance.

Fig. 9 shows the diurnal variation of heat balance on the water body thus obtained. The sensible heat fluxes H is relatively small during the day, and it moves towards the water body, which is the major agency to cool air flow while it crosses the water surface. Most amount of the net radiation R_{net} is transferred to G on the water body, and it implies that the river can store a

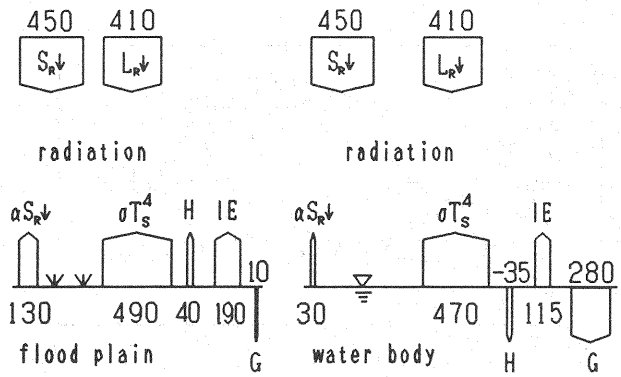

Fig. 10 Schematic diagram of heat balance on the flood plain and the water body at the time $14h$ (Unit :W/m^2).

large amount of heat without raising its water temperature though the depth is relatively small (about $8m$ at location c).

(iii) Characteristics of the heat balance of the river course

A schematic diagram of heat balance on the flood plain and the water body at the time $14h$ is shown in Fig. 10, in which the downward radiations are assumed to be identical on both surfaces, because they were not measured on the boat. The difference in the upward short-wave radiations were caused by the difference in albedo. The difference of the upward long-wave radiations is due to the difference in surface temperatures. The net radiation R_{net} is distributed to H, ℓE and G as described in the above. The latent heat flux ℓE is predominant on the flood plain among these quantities, and G is very large on the water body. On both surfaces, the amount of H is found to be small. The average of heat balance during $5h$ and $18h$ shows that 50 % of the R_{net} was changed to ℓE on the flood plain, and 80 % of the R_{net} was converted to G for the water body.

The diurnal change of H and ℓE on both surfaces (see Figs. 7 and 9) indicates that H and ℓE on the water body were smaller in the daytime($7h \sim 18h$) than that on the flood plain, and an inverse situation occurred after the sunset($18h \sim 20h$). Thus, it is expected that the water body is effective to improve the heat environment in the daytime and the flood plain after the sunset, if we assume that the improvement of the micro-climate near the river course is achieved on the condition that the temperature and humidity are reduced.

The temperature of the lower atmosphere is mainly affected by the sensible heat flux H. The amount of atmospheric cooling on the river course is proportional to the difference of sensible heat fluxes inside and outside the river course, as described before in Fig. 4. Since the sensible heat flux was not measured in the city region in the present observation, we employ the result of measurements made by Asaeda and Fujino (Ref. 7), who reported that the maximum sensible heat fluxes on asphalt pavement and concrete pavement become 350 and 160 W/m^2, respectively, in summer. Comparing the values cited and the observed values in the present study, the sensible heat flux on the flood plain (maximum value during the observation : $100W/m^2$) and that on the water body (during the observation ≈ 0) are considerably smaller than that in the city region.

CONCLUDING REMARKS

The process of the atmospheric cooling above the river course was studied based on the heat and meteorological observation. The results are :

(1) Distinct developments of internal boundary layers of momentum and heat were observed for the wind which crosses the river course. The air flow in the lower atmosphere was cooled by the river course, and the effect extends to a height of $30m$ at maximum.

(2) The rate of heat exchange(= cooling of the atmosphere) becomes large in the afternoon compared with that observed in the morning.

(3) The role of the flood plain and the water body in cooling of the atmosphere was studied based

on the heat balance analysis. The sensible heat flux H on the both surfaces was small during the day, which is the main agency of the atmospheric cooling. The latent heat flux ℓE on the flood plain and the heat flux G into the water body are predominant in the heat balance.

Acknowledgments: The authors are indebted to the members of River Environment Research Division of Public Works Research Institute, Hydraulic Engineering Laboratory of Tokyo Institute of Technology and Ara–river Lower Reach Work Office of Kanto Regional Construction Bureau, Ministry of Construction, who assisted with the field observation. Mr. Shimatani, Director of the River Environment Division of Public Works Research Institute, is greatly acknowledged with his valuable suggestions and arrangements during the observation. The present study is financially supported by a Grant–in–Aid for Scientific Research from the Ministry of Education and Culture of Japan(grants 04750492) and by a grant offered from Andoh Foundation.

REFERENCES

1. Pielke, R. A. : Mesoscale meteorological modeling, Academic Press, pp.482–492, 1984.

2. Kawamura, T. : Urban atmospheric environment (in Japanese), Tokyo University Press, pp.1–42, 1979.

3. Yoshino, M. : The role of water body in the urban climate (in Japanese), Journal of Architecture and Building Science, Vol.98, No.1208, pp.42–45, 1983.

4. Bolton, D. : The computation of equivalent potential temperature, Monthly Weather Review, Vol.108, pp.1046–1053, 1980.

5. Takewaka, S., S. Ikeda, T. Hirayama, Y. Kayaba and T. Zaitsu : Meteorological environment in surrounding region of urban rivers (in Japanese), Journal of Hydraulic, Coastal and Environmental Engineering, JSCE, No.479, pp.11–20, 1993.

6a. Brutsaert, W. : Evaporation into the atmosphere, Kluwer Academic Publishers, pp.128–153., 1982.

6b. ditto, pp.197–207.

6c. ditto, pp.190–193.

7. Asaeda, T. and T. Fujino : Heat flux and heat storage properties of the paved ground (in Japanese), Journal of Japan Society of Hydrology & Water Resources, Vol.5, No.4, pp.3–7, 1992.

APPENDIX - NOTATION

The following symbols are used in this paper :

U	=	horizontal wind velocity;
V	=	vertical wind velocity;
T	=	air temperature $[^oC]$;
RH	=	relative humidity [%];
q	=	vapor density $[g/m^3]$;
WD	=	wind direction;
ρ	=	air density;
C_p	=	specific heat for constant pressure;
L_F	=	width of the river course;

f_c = sensible heat flux at the surface in city region;
f_r = sensible heat flux at the surface in the river course;
F', F = amount of heat exchange above the river course;
H = sensible heat flux at the surface;
E = water vapor flux at the surface;
ℓ = latent heat of vaporization;
ℓE = latent heat flux at the surface;
G = sensible heat flux below the surface;
σ = Stefan-Boltzman constant;
T_s = surface temperature;
σT_s^4 = upward long-wave radiation emitted from the surface;
$S\downarrow$ = downward short-wave radiation;
$L\downarrow$ = downward long-wave radiation;
α = albedo of the surface;

subscripts

d = value measured at the downwind location;
u = value measured at the upwind location;
w = value of the water body;
$soil$ = value in the soil layer;